Locatelli *et al. Cardiovascular Diabetology* (2026) 25:34
https://doi.org/10.1186/s12933-025-03046-3

Cardiovascular Diabetology

REVIEW Open Access

# Impacts of ketogenic diet intervention on cardiometabolic outcomes in obese, dysglycemic mice

Cassandra A. A. Locatelli[1,2], My-Anh Nguyen[1,2], Nadya M. Morrow[1,2], Elena Cameron[2,3], Natasha A. Trzaskalski[1,2], Ilka Lorenzen-Schmidt[2], Arianne Morissette[2] and Erin E. Mulvihill[1,2,4,5*]

## Abstract

**Background** The ketogenic diet (KD) is widely recognized for its potential benefits in individuals with type 2 diabetes, but findings from both human and animal studies remain inconsistent. Type 2 diabetes is often comorbid with liver steatosis and atherosclerosis which are characterized by inflammation and dysregulated lipid metabolism. Moreover, whereas KD has shown mixed, sometimes detrimental, effects on circulating cholesterol levels in humans, it is currently unclear the whole-body balance of risk and benefit across hepatic, atherosclerotic, and pancreatic effects.

**Methods** We used lean, diet-induced obese, and diet-induced obese, atherosclerotic (PCSK9 overexpression (OE)) mouse models to assess the impact of an extreme KD on cardiometabolic outcomes. Obese and PCSK9 OE mice received 10 weeks of cholesterol-supplemented HFD before 12 weeks of KD intervention whereas lean mice received KD, chow, or HFD for 12 weeks.

**Results** KD intervention induced weight loss in obese female and PCSK9 OE male mice, but not male, wildtype mice. Across models, KD did not improve glucose tolerance or ex vivo insulin secretion, despite elevated levels of insulinotropic GLP-1 after glucose gavage. Pancreas lipids were similar between diet groups in obese mice, but liver steatosis or inflammation were generally improved in all models on KD. All KD groups had increased hepatic expression of genes for fatty acid oxidation, ketone body production, and ketone utilization. KD-intervened PCSK9 OE mice had lower circulating TNFα and chemokines (CCL2, CCL4, CXCL1, CXCL2) as well as smaller atherosclerotic lesion area relative to mice that continued on the HFD. The PCSK9 OE male mice on KD intervention also had reduced circulating LDL cholesterol but this effect was lost in mice with intact LDL receptor signaling, which also had fasting hypertriglyceridemia in line with HFD continuers.

**Conclusions** This study demonstrates that, in mice, a high cholesterol KD can improve hepatic steatosis particularly when weight loss is achieved, compared to maintaining the western-style HFD. However, no improvements to insulin secretion and glucose tolerance were observed despite elevated post-glucose GLP-1 levels and long-term diminished requirements for insulin.

**Keywords** Ketogenic diet, Islets, Glucagon like peptide 1-, Steatosis, Atherosclerosis, Cholesterol, Inflammation

*Correspondence:
Erin E. Mulvihill
emulvihi@uottawa.ca

Full list of author information is available at the end of the article

## Background

The first line treatment for cardiometabolic diseases like type 2 diabetes (T2D) and obesity is dietary manipulation, which can include the recently re-emerged, ketogenic diet (KD). The KD is an extremely high fat (> 70% of calories), and low carbohydrate (< 10% of calories) diet that can elevate ketone bodies in circulation, inducing a metabolic state called ketosis. This diet has shown benefits in short-term human studies of people living with T2D by reducing body weight, improving blood glucose management, and reducing the requirements for T2D medications [1]. Whether this effect is due to improved pancreatic islet function or tissue insulin sensitivity versus reduced insulin requirement has not been fully elucidated.

Physiological glucose control is regulated by tissue sensitivity to insulin, insulin secretion, and postprandial intestinal signals. The incretins, glucagon-like peptide-1 (GLP-1) and glucose dependent insulinotropic polypeptide (GIP) are released from the specialized small intestinal cells in response to nutrients, including glucose and lipids [2]. At the islet, GLP-1 and GIP amplify glucose stimulated insulin secretion (GSIS) through G-protein coupled receptor (GPCR) signaling, unless they are inactivated by dipeptidyl peptidase-4 (DPP4) [3]. Similarly, fatty acids and ketones can signal through islet GPCRs to amplify or modulate GSIS [4, 5].

Aside from ketones, the extreme fat consumption of a KD raises questions about the impact on T2D comorbidities like obesity and atherosclerotic cardiovascular disease as well as the direct effects on the pancreatic islet and tissue storage of the ingested lipids. Dietary fat intake, particularly of saturated fatty acids, has long been associated with increased low-density lipoprotein (LDL) cholesterol, a major risk factor for cardiovascular disease like atherosclerosis [6, 7]. Even the impact of KD-induced extreme elevations in cholesterol have resulted in controversial effects on atherosclerosis in people [8]. Further, diet can alter the presence of inflammatory markers in circulation, including atherogenic cytokines and chemokines interleukin 1β (IL-1β), keratinocyte chemoattractant/growth-regulated oncogene (KC-GRO aka CXCL1), tumor necrosis factor α (TNFα), monocyte chemoattractant protein 1 (MCP-1 aka CCL2), and interleukin 6 (IL-6) [9–14]. Despite concerns that the extremely high fat content of a KD may elevate the risk of cardiometabolic diseases through inflammation and increased LDL cholesterol, evidence from both human and animal studies remains controversial with dietary fat composition and genetic susceptibility (e.g., familial hypercholesterolemia) being important factors in individual risk [15–17].

Cardiometabolic diseases are characterized by both dyslipidemia and inflammation. Our group previously showed that in lean male mice, 3 weeks of KD feeding increases intestinal triglyceride secretion after a dietary fat challenge, which may contribute to pro-atherogenic dyslipidemia [18]. Recent studies in lean *ApoE*$^{-/-}$ mice have shown that KD feeding can induce atherosclerosis compared to low fat control diets [19, 20] but does not increase inflammation and plaque size to the same extent as HFD controls [21]. Raising beta-hydroxybutyrate (BHB) levels, by direct administration in HFD-fed *ApoE*$^{-/-}$ mice or with SGLT2i medications in individuals living with T2D, dampens inflammatory IL-1β and TNFα levels [22–24].

Importantly, the available evidence in rodents shows that KD worsens glucose tolerance in lean mice but may have benefit in diet or genetically induced obese mice [25–27]. While individuals may lose liver fat on a KD [28–30], studies in lean mice indicate worse liver outcomes [31–33] whereas mice with established metabolic dysfunction-associated steatotic liver disease given a KD had lower liver weight and triglycerides than HFD-fed mice [34]. These discrepancies highlight the need for a more comprehensive understanding of the KD's effects across cardiometabolic disease models and outcomes, using both low- and high- fat diet controls, particularly in the context of pre-existing metabolic dysfunction for translational purposes.

We directly tested the effects of the same KD formulation across multiple preclinical models to systematically assess the impact of model selection on observed outcomes. We used models of lean mice, diet induced obese mice, as well as diet induced obese, atherosclerotic mice to investigate the effects of the KD on glucose response and insulin secretion, inflammation, lipid metabolism and storage, and atherosclerosis progression.

## Methods

### Animals and diets

Male and female C57BL6/J were housed on 12 h light dark cycle at 20–22˚C. Food was administered ad libitum unless fasting was indicated; mice had free access to water. All mice were fed a grain-based diet regular chow (chow; Envigo 2019) until 10 weeks of age. From there: intervention model mice were given a high fat diet with supplemented cholesterol (HFD; Envigo TD88137) for 10 weeks then, for the following 12 weeks were given a diet "intervention" of our custom KD (Envigo TD190587; previously published (18)), regular chow (Envigo 2019 Teklad Global 19% Protein Extruded Rodent Diet), or maintenance on the HFD. A subset of intervention mice (PCSK9 OE) were administered proprotein convertase subtilisin/kexin type 9 (PCSK9) overexpressing adeno-associated virus (AAV8.HCRAApoE.hAAT.mPCSK9.D377Y.bGH Addgene 68376) developed by Pennsylvania (Penn) Vector Core at a titre of $1 \times 10^{11}$ at day zero of HFD feeding to allow the development of atherosclerosis

and followed the intervention diet protocol (35). No induction mice continued to receive chow diet until the diet switch where they received KD, chow, or HFD for 12 weeks until endpoint. Animal care followed all guidelines from the Canadian Council on Animal Care and procedures were approved by the University of Ottawa Animal Care Committee.

#### Body composition analysis

EchoMRI (EchoMRI-100 machine, Echo Medical Systems, Houston, TX, USA) was used to measure lean and fat mass in awake mice.

#### Glucose and insulin tolerance tests

Mice were fasted for 4–5 h before glucose gavage (2 g/kg) or intraperitoneal insulin injection (0.6 IU/kg Humalog Eily Lilly VL7533, DIN: 02229704) and subsequently bled by tail snip every 15 min for 90 min. StatStrip Xpress Blood Glucose Meter was used to measure blood glucose over time and blood was collected for plasma at 0 and 15 min for glucose tolerance test (GTT).

#### Blood and plasma collection

Blood glucose and BHB were measured with StatStrip Xpress Blood Glucose Meter and with FreeStyle Precision Neo, respectively. Blood was collected in EDTA coated capillary microvette tubes (Sarstedt Microvette CB300K2E) and centrifuged for 10 min at 12,000 rpm (13500 rcf) and 4˚C. Plasma was stored at -80˚C until analyses were performed (Mouse Active GIP Elisa Kit; Crystal Chem 81511, V-PLEX GLP-1 Active Kit Mesoscale K15030D, Ultra Sensitive Mouse Insulin ELISA Kit-ALPCO 80-INSMSU-E01, U-PLEX Chemokine Combo 1 (mouse); Mesoscale K15321K, V-PLEX Proinflammatory Panel 1 Mouse Kit Mesoscale K15048D, Glucagon ELISA Mercodia 10127101, Mouse Glucagon ELISA kit CrystalChem 81518). For plasma collected for active GLP-1 and active GIP quantification, Trasylol (5000 KIU/mL), EDTA (1.2 mg/mL), Diprotin A (0.1 nmol/L) was added. Liver (ALT, AST, ALP) and cardiovascular (cholesterol, HDL, LDL, glucose) panels were run by the pathology core at The Centre for Phenogenomics. Plasma bile acid quantification was done using LC–MS/MS at Infectious and Immune Diseases Research Axis, Centre de Recherche du CHU de Québec-Université Laval as previously described [36]. Fatty acid quantification was done by GC/MS at Metabolomics Core Facility Faculty of Medicine, University of Ottawa. Due to cohort differences in some fatty acid concentrations, total fatty acid levels were normalized to HFD continuer controls for each cohort.

#### Tissue collection

Mice were sacrificed with (1 pm) or without (8 am) 5 h of fasting under isofluorane or $CO_2$ (PCSK9 OE) inhalation and underwent cardiac puncture for blood collection. Tissues for gene expression, protein quantification (Pierce Rapid Gold BCA Protein Assay Kit A53225, R&D Systems Mouse LDLR Quantikine ELISA Kit MLDLR0, R&D Systems Mouse Proprotein Convertase 9/PCSK9 Quantikine ELISA Kit MPC900), and lipid measurements were snap frozen and stored at -80˚C. PCSK9 OE mice were perfused with saline through the left ventricle. Aorta were cleaned and the root and liver tissue were embedded in OCT (TissueTek) and frozen for histology. The remaining aortas (arch to iliac bifurcation) were snap frozen in liquid nitrogen and stored at -80C. In mice undergoing portal duct cannulation, they were fasted overnight and given a glucose gavage (2 g/kg) 15 min prior to portal vein cannulation and blood collection under isofluorane anesthesia. In these mice, pancreas is snap frozen for lipid quantification.

#### Tissue lipid quantification

Tissue lipids were extracted using modified Folch method in obese (pancreas and liver) [37] and PCSK9 OE (liver) [38] as previously described. Extracted cholesterol and triglycerides were measured using Infinity™ Cholesterol Liquid Stable Reagent (Thermo Scientific TR13421) and Infinity™ Triglycerides Liquid Stable Reagent (Thermo Scientific TR22421).

#### Islet isolation and perifusion

For islet isolation, pancreases were inflated with collagenase (7.5 mg/mL, SigmaC7657) in Hanks Balanced Salt Solution (5 mM glucose, 1 mM $MgCl_2$). Then pancreases were kept on ice until heating at 37 ˚C for 12 min. Then, digested pancreases were shaken vigorously and washed with Hanks Balanced Salt Solution (5 mM glucose, 1 mM $MgCl_2$, 1 mM $CaCl_2$). Islets were separated by Histopaque (Sigma, 10771) gradient, hand-picked for purity, and rested overnight in RPMI (10% FBS, 1% penicillin/streptomycin) at 37˚C and 5% $CO_2$.

Solutions for perifusion, GLP-1 (GLP-1 7–36, Bachem, 4030663), GIP (GIP-(D-Ala2)-GIP, Bachem 4054476), and KCl were made with KRBH buffer (115 mM NaCl, 5 mM KCl, 2.5 mM $CaCl_2$, 24mM $NaHCO_3$, 10 mM HEPES, and 1% BSA; pH = 7.4). Using the Biorep perifusion machine, 80 islets per mouse were equilibrated for 45 min at 2.8 mM glucose before stimulation with solutions. Temperature (37˚C) and flow rate (100 µL/min) were kept constant, and effluents were collected every 2 min. Effluent insulin concentration was measured with Mouse Ultrasensitive or High Range Insulin ELISA (ALPCO, 80-INSMSU-E01 or 80-INSMSH).

#### Gene expression

Liver RNA was isolated and cDNA was reverse transcribed with TRIzol Reagent (Ambion) and

High-Capacity cDNA Reverse Transcription Kit (Fisher Scientific 43-688-14), respectively, per manufacturers protocols. mRNA quantity was determined with TaqMan Fast Advanced Master Mix (Applied Biosystems 4444557) using standard curve method (Quantstudio 5) and was normalized to *Ppia* or *Tbp*. Aorta RNA was isolated with TRIzol Reagent (Ambion) and prepared for Nanostring gene expression analysis using manufacturers protocol.

#### Nanostring gene expression analysis

Inflammatory gene and pathway analyses were done using the Nanostring nCounter® Mouse Inflammation Panel with 100 ng of aorta RNA. Capture and reporter probes were hybridized with the RNA for 16 h at 65 °C. Assays were performed on the nCounter system per manufacturer's instructions. Intervention diets were analyzed with HFD continuers as the baseline. Benjamini-Hochberg p-value correction was used for false discovery rate.

#### Histological analyses

Serial sections of the aortic sinus, starting at the origin of the aortic valves, were sectioned at a thickness of 10 µm on a cryostat (Leica CM3050S) as were sections of liver. Sections were stained with Oil Red O for 12 min at 60°C or haematoxylin and eosin for 5 min each at room temperature. Photomicrographs were obtained using a slide scanner (Leica Aperio Versa). Atherosclerotic lesion size was quantified by an individual blinded to the treatment group as an average of 4–8 sections on 2 slides using ImageJ. ImageJ was used to quantify red pixels in liver tissue stained with Oil Red O.

#### Statistical analysis

Data are presented as mean ± SEM and statistical analyses were done in Graphpad Prism 10. Significant differences between groups were determined using unpaired t-test (2 groups) or one-way ANOVA with multiple comparisons (3 groups). Nanostring statistical analyses are described above. Measures taken over time were analyzed with two-way ANOVA with Tukey's (between 3 groups) or Šídák's (between two groups) multiple comparisons.

## Results

#### KD intervention sustains fasting-like plasma metabolite profile through refeeding

Wildtype male and female mice were separated into two diet protocols. The first protocol, the induction-intervention group, was designed to model established metabolic dysfunction as often seen in individuals living with T2D. Mice were given a HFD from 10 weeks of age for 10 weeks prior to an intervention of regular chow or KD for 12 weeks before sacrifice (Fig. 1A). As a control, "HFD continuers" continued on the HFD for the 12-week intervention period. The second protocol used a lean no induction group, which replicates conditions often used in mouse studies of the KD. Mice received HFD, chow, or KD at 20 weeks of age for 12 weeks (Fig. 1A). The KD was designed using the same ingredients as the HFD, high in saturated fat and cholesterol [18], with altered proportions in line with the diet conventions to not bias for a "healthier" KD (Supplemental Table 1).

After 2 weeks of diet intervention, average food intake was similar among diet groups (Fig. 1B). KD intervention had no impact on body weight in male intervention mice but caused significant weight loss in female intervention mice compared to HFD controls (Fig. 1C, D). In both sexes, average energy efficiency in the first two weeks of KD intervention trended lower than HFD continuers (Supplemental Fig. 1A, B). KD feeding had no significant effect on total body mass in the leaner male and female no induction mice (Fig. 1E, F). During week 10 of diet intervention, the mice were fasted overnight before being refed their respective diet. Blood was taken after 16 h fast to ensure consistently elevated ketones across groups and 2 h post-refeed to evaluate the flux of circulating metabolites across fasting and fed states and the fasting-like quality of the KD [39]. KD intervention males maintained stable blood BHB and glucose, plasma free fatty acids (FFA), insulin, and glucagon levels from 16 h fasted to 2 h refed states (Fig. 1G-K). Plasma insulin was not significantly different among KD intervention and HFD continuer males during fasting or refeeding (Fig. 1J) and refed glucagon was significantly lower than HFD continuers (Fig. 1K). In females, blood and plasma metabolite levels were more stable after refeeding with KD intervention than HFD, with some changes (Fig. 1L–P). Females on KD intervention had lower BHB levels after refeeding than at 16 h fasted, but these levels were still significantly higher than the other diet groups and well within the range of nutritional ketosis (> 0.5 mM) [1] (Fig. 1L). Female KD intervention mice had lower blood glucose after refeeding than chow and HFD mice, maintained high FFA levels, but significantly increased glucagon levels with refeeding (Fig. 1M–P). In lean "no induction" mice, KD fed mice had significantly higher blood BHB levels but no difference in blood glucose in both males and females (Fig. 1Q-T). Taken together, this KD induced a fasting-like state with circulating metabolites but only induced weight loss in female, intervention mice.

#### KD feeding does not alter stored pancreas lipids or islet GSIS but reduces glucagon at low glucose

Since glucose stimulates the release of lipids stored in the intestine [40, 41], we assessed the circulating post-glucose lipid environment by performing portal vein

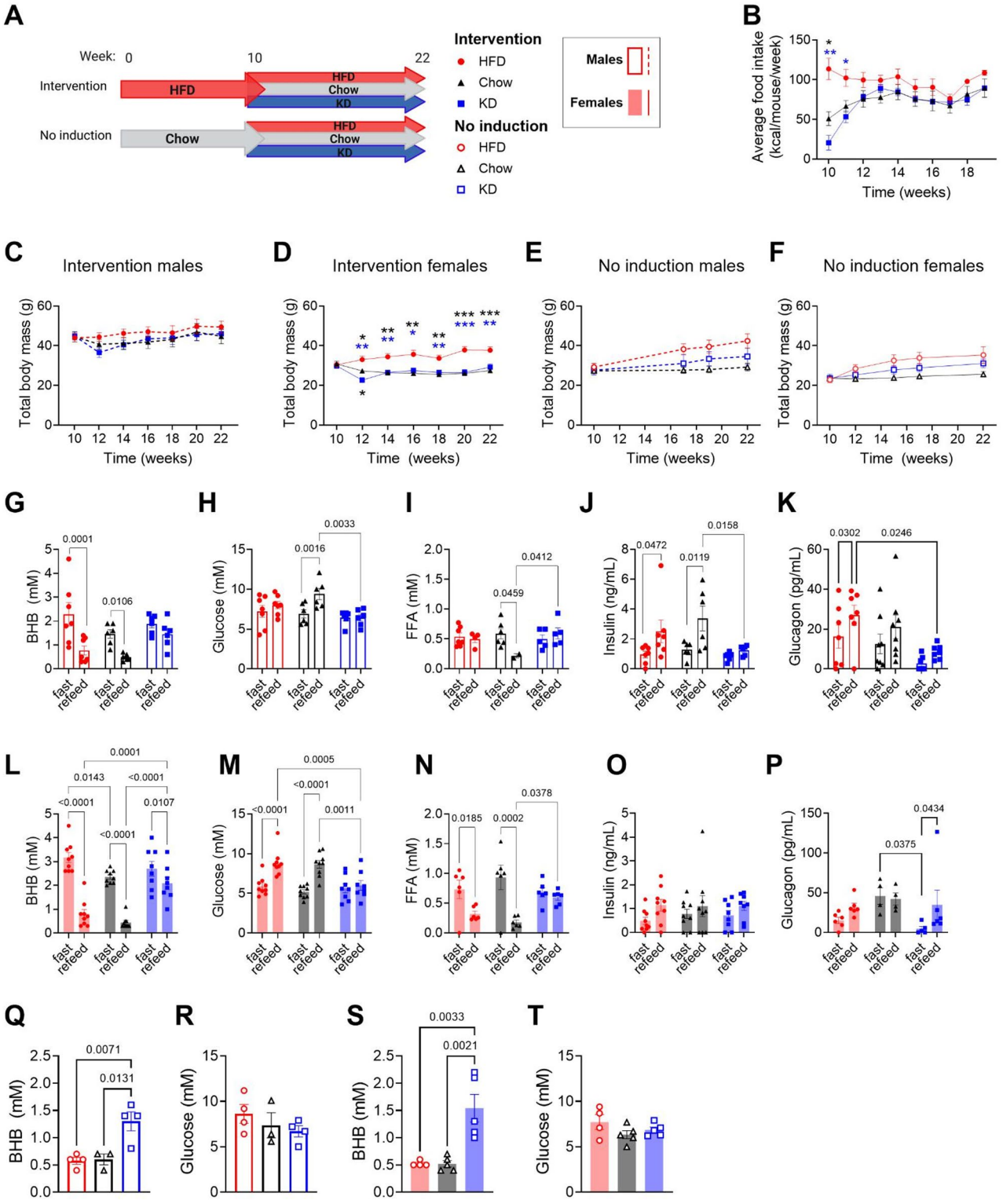


**Fig. 1** KD intervention maintains fasting plasma metabolites in the fed state. **A** Schematic of experimental protocol, **B** weekly food intake averaged from group housed male and female intervention mice, **C**–**F** total body mass over time in male (**C**) and female (**D**) intervention and male (**E**) and female (**F**) no induction mice, (**G**–**K**) Blood BHB and glucose, and plasma FFA, insulin, and glucagon after 16 h fast and 2 h refeeding of their respective diets in male intervention mice, (**L**–**P**) Blood BHB and glucose, and plasma FFA, insulin, and glucagon after 16 h fast and 2 h refeeding of their respective diets in female intervention mice. (**Q**–**R**) Fed BHB and glucose in no induction male mice. (**S**–**T**) Fed BHB and glucose in no induction female mice. Data are presented as mean +/− SEM. P value was determined by two way ANOVA with multiple comparisons (**B**–**P**). or one way ANOVA with multiple comparisons (**Q**–**T**).

cannulation 15 min after glucose gavage. Gas chromatography mass spectrometry (GC/MS) identified 26 fatty acids in portal vein plasma. Relative to HFD continuers, KD intervention males had lower total measured plasma fatty acids (Fig. 2A). The saturated fatty acid lauric acid methyl ester (12:0) was not different from HFD continuers in KD intervention males in portal vein plasma, nor was the monounsaturated alpha linoleic acid methyl ester (18:3n3), which was highest in chow intervention males (Fig. 2B, C). Cis-11,14 ecoisanoidenoic methyl ester (20:2), a polyunsaturated fatty acid, was significantly lower in both intervention groups than male HFD continuers (Fig. 2D). Biochemical determination of pancreas triglycerides and cholesterol levels were not different among diet groups in male intervention mice (Fig. 2E, F). In KD intervention females, total portal vein fatty acids were also significantly lower than HFD continuers (Fig. 2G). The saturated fatty acid lauric acidy methyl ester (12:0) trended lower with KD intervention relative to HFD continuers in females ($p$ = 0.055) (Fig. 2H, I). The unsaturated fatty acids alpha linoleic acid methyl ester (18:3n3) and cis-11,14 ecoisanoidenoic methyl ester (20:2) followed the same effect as males, unchanged and lower than HFD continuers, respectively (Fig. 2J). Pancreas triglycerides and cholesterol levels were not different among diet groups in female intervention mice (Fig. 2K, L).

After 6 weeks of intervention, KD did not alter glucose tolerance compared to HFD continuer males (Supplemental Fig. 2A). However, KD intervention male mice had significantly lower plasma insulin at fasting and after glucose gavage compared to HFD continuers (Supplemental Fig. 2B). KD intervention males had significantly higher plasma active GIP and GLP-1 levels post glucose (Supplemental Fig. 2C-D). Although not statistically significant, KD intervention males had lower mean plasma glucagon levels (fasted $p = 0.079$) (Supplemental Fig. 2E). Female KD intervention mice had the highest glycemia during the glucose tolerance test (GTT) and significantly lower post-glucose insulin than HFD continuers (Supplemental Fig. 2F, G). Female KD intervention mice had unchanged plasma active GIP levels, but significantly higher plasma active GLP-1 levels compared to HFD continuers (Supplemental Fig. 2H, I). Fasting glucagon levels were significantly lower in KD intervention females relative to HFD continuers (Supplemental Fig. 2J). Therefore, despite higher plasma active GLP-1 levels, glucose homeostasis was not improved with KD intervention in male and female mice, respectively. After 6 weeks of KD feeding, the no induction males and females had similar glucose tolerance between diets, but KD-fed mice had the highest active GIP and GLP-1 (Supplemental Fig. 2K-P). Insulin tolerance was not significantly different between diet groups in either diet protocol or sex (Supplemental Fig. 2Q-T).

We performed perifusion in isolated islets from intervention and no induction mice to test the islet secretory capacity in isolation of other physiological factors. Both male and female intervention groups had similar GSIS among diet groups in response to high glucose, GLP-1, GIP, and KCl during the dynamic perifusion experiment (Fig. 2M, N). As expected, high glucose significantly lowered perfusate glucagon levels across diet groups (Fig. 2O, P). However, glucagon measured during perifusion low glucose was significantly lower in islets from KD intervention male and female mice than islets from HFD continuers (Fig. 2O, P). Similarly, islets from no induction male and female KD mice had similar GSIS responses to the other diet groups; but no induction KD islets, particularly from females, were more likely to have very high islet GLP-1 release than HFD and chow-fed mice (Fig. 2Q–T). Thus, this KD elevated active GLP-1 and reduced glucagon but does not improve insulin response to glucose.

### KD intervention protects against liver lipid accumulation in lean and obese female mice

Liver mass trended lower ($p = 0.057$) in male KD intervention mice compared to HFD continuers (Fig. 3A). While liver triglycerides were unchanged, liver cholesterol mass was significantly lower with KD intervention compared to HFD continuers (Fig. 3B, C). Female KD intervention mice, however, had lower liver weight, triglycerides, and cholesterol relative to HFD continuers (Fig. 3D–F). Plasma levels of liver enzymes alanine transaminase (ALT), aspartate aminotransferase (AST), and alkaline phosphatase (ALP) were lower with KD intervention in males but only ALT was significantly lower in intervention females (Fig. 3G–L). Gene transcript levels associated with ketone production (3-hydroxy-3-methylglutaryl-CoA synthase 2 (*Hmgcs2*)) and interconversion (D-beta-hydroxybutyrate dehydrogenase (*Bdh1*)), as well as fatty acid oxidation (carnitine palmitoyltransferase I (*Cpt1α*)) were significantly higher in KD intervention male and female mice (Fig. 3M–R). In no induction mice, KD-fed males had insignificantly different liver weight, triglycerides (trend $p = 0.0627$ KD and HFD), and cholesterol whereas females had significantly lower total liver weight and liver triglycerides (Fig. 3S–X). Again, KD feeding significantly increased hepatic expression of *Hmgcs2*, *Bdh1*, and *Cpt1α* (Fig. 3Y–AD). Together, across lean and obese models, the KD reduced markers of hepatic inflammation and/or lipid stores.

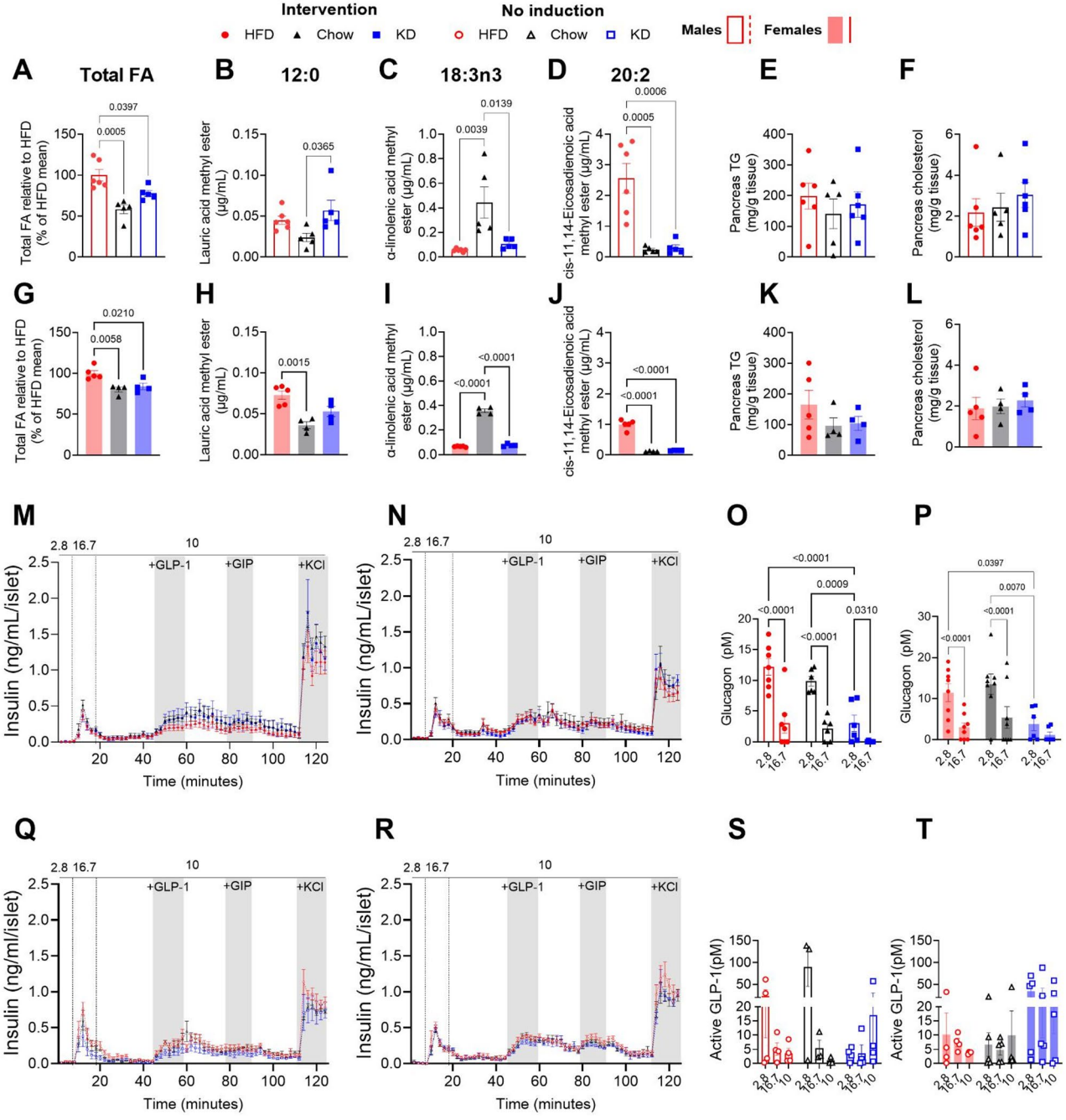


**Fig. 2** KD feeding does not alter stored islet lipids or GSIS but reduces glucagon at low glucose. **A** Total quantification of portal vein fatty acids relative to the average total fatty acids of HFD mice per cohort in intervention males, **B**–**D** quantification of fatty acids from portal vein plasma 15 min after glucose gavage in male intervention mice, **E**, **F** pancreas TG and total cholesterol in male intervention mice, **G** total quantification of portal vein fatty acids relative to the average total fatty acids of HFD mice in intervention females. (**H**–**J**) Quantification of fatty acids from portal vein plasma 15 min after glucose gavage in female intervention mice, **K**–**L** pancreas TG and total cholesterol in female intervention mice, **M**, **N** GSIS during perifusion in islets isolated from male (**M**) and female (**N**) intervention mice, (**O**–**P**) Glucagon measured at 2.8 mM and 16.7 mM glucose during perifusion of islets isolated from male (**O**) and female (**P**) intervention mice, (**Q**, **R**) GSIS during perifusion in islets isolated from male (**Q**) and female (**R**) no induction mice, (**S**, **T**) Active GLP-1 measured at 2.8 mM, 10 mM, and 16.7 mM glucose during perifusion of islets isolated from male (**S**) and female (**T**) no induction mice. Data are presented as mean +/− SEM. P value was determined by two way ANOVA with multiple comparisons (**M**–**T**) or one way ANOVA with multiple comparisons (**A**–**L**).

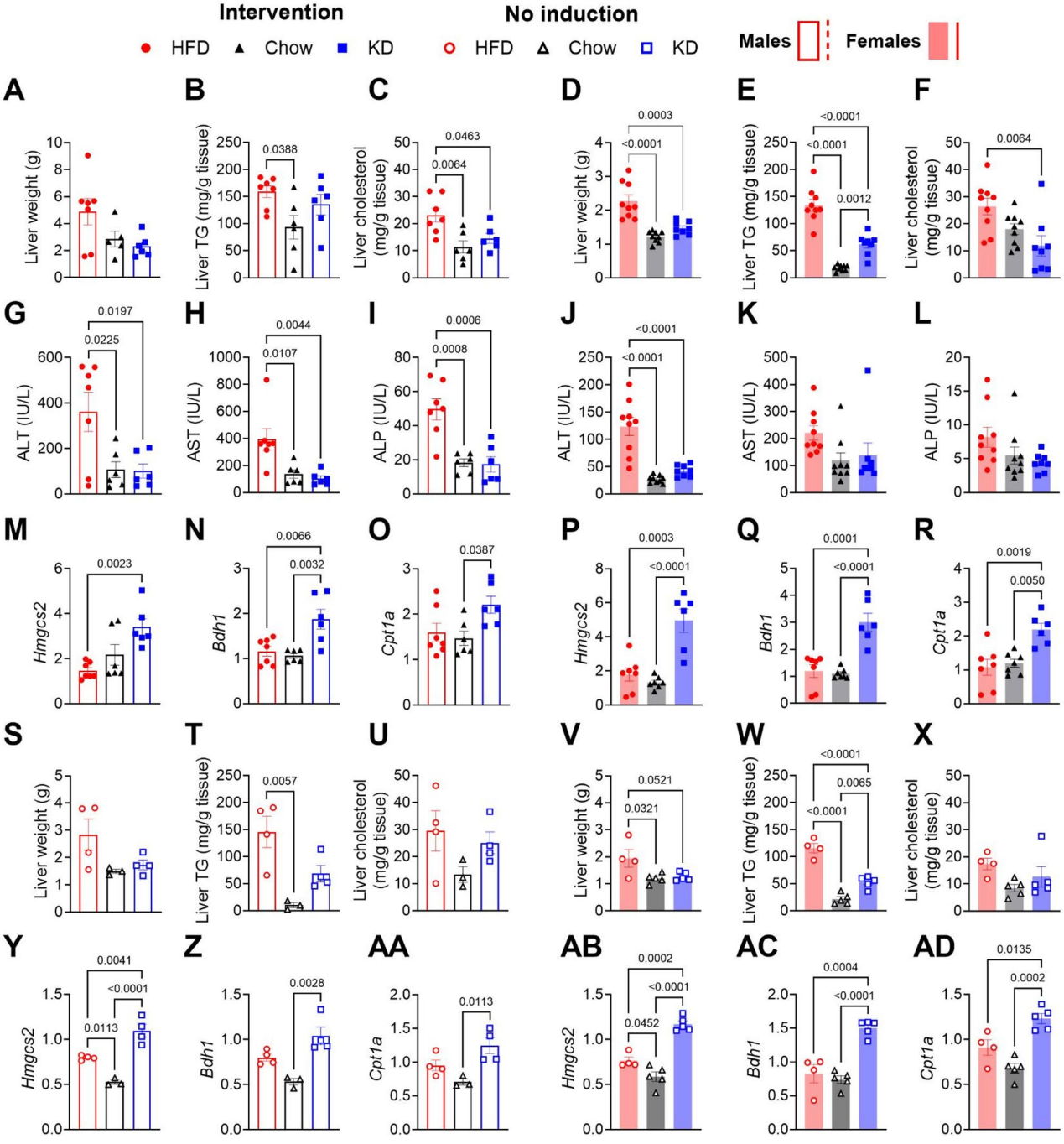


**Fig. 3** KD intervention protects against liver lipid accumulation with metabolic transcriptional changes. (**A**–**C**) Endpoint total liver mass, liver TG, and total liver cholesterol in male intervention mice. (**D**–**F**) Endpoint total liver mass, liver TG, and liver total cholesterol in female intervention mice. (G-I) Plasma liver enzymes in fed endpoint plasma of intervention males. (**J**–**L**) Plasma liver enzymes in fed endpoint plasma of intervention females. (**M**–**O**) Relative gene expression normalized to *Ppia* in livers from intervention males. (**P**–**R**) Relative gene expression normalized to *Ppia* in livers from intervention females. (**S**–**U**) Endpoint total liver mass, liver triglycerides, and liver cholesterol in no induction male mice. (V-X) Endpoint total liver mass, liver triglycerides, and liver cholesterol in no induction female mice. (**Y**–**AA**) Relative gene expression normalized to *Ppia* in livers from no induction males. (AB-AD) Relative gene expression normalized to *Ppia* in livers from no induction females. Data are presented as mean +/− SEM. P value was determined by one way ANOVA with multiple comparisons.

### KD intervention reduces markers of inflammation and liver lipids in obese, atherosclerotic mice

To assess the impact of the KD intervention on atherosclerosis, we administered PCSK9 overexpression (PCSK9 OE) AAV before HFD induction for the intervention diet protocol in males. Overexpression of pAAV/D377Y-mPCSK9 leads to hypercholesterolemia through rapid degradation of the LDLR and allows for development of atherosclerotic lesions in the aortic root and arch in mice on high cholesterol diets without germline deletion of the LDLR or ApoE [35]. PCSK9 OE diminished hepatic LDLR protein levels 10–20 fold relative to the wildtype female and male mice (Supplemental Fig. 3A–C). The 10-week HFD induction period reliably increased circulating cholesterol levels in PCSK9 OE males and allowed for the initiation of atherosclerosis before diet intervention (Supplemental Fig. 3D–F). PCSK9 OE did not impact ketosis or food intake (Supplemental Fig. 3G, H). KD intervention in PCSK9 OE males did, however, induce loss of total body weight through the loss of fat mass (Supplemental Fig. 3I–K). The change in body weight relative to kcal intake trended lower than HFD continuers, potentially indicating mildly increased energy expenditure or reduced metabolic efficiency in the diet transition period (Supplemental Fig. 3L). After a 4-hour fast, KD intervention mice had lower circulating DPP4 protein levels and activity, as well as lower circulating insulin (Supplemental Fig. 3M–O). During a GTT, KD intervention PCSK9 mice had lower insulin levels and higher active GLP-1, but not GIP, after glucose gavage (Supplemental Fig. 3P-R). Consistent with greater small intestinal length observed with short term KD feeding [18] and the effect of greater GLP-1 levels [42], KD intervention mice had significantly greater small intestinal length than HFD continuers (Supplemental Fig. 3S).

KD intervention in PCSK9 OE mice significantly reduced liver triglycerides and cholesterol relative to HFD-continuers and resulted in significantly reduced neutral lipid staining on hepatic histological slices (Fig. 4A–D). Circulating liver enzymes, ALT and ALP, but not ALP, were also significantly lower in KD intervention mice compared to HFD continuers (Fig. 4E–G). Hepatic transcript levels of total, pro-resolving, and pro-inflammatory macrophage markers *Adhesion G protein-coupled receptor E1* (Adgre*1*), *Mannose receptor C-type 1 (Mrc1)*, and *Integrin subunit alpha X* (*Itgax*) were significantly lower in KD intervention than HFD mice sacrificed in the fed state (Fig. 4H–J). KD intervention PCSK9 OE mice also had elevated *Hmgcs2* mRNA levels, like non PCSK9 OE mice, but not significantly different *Cpt1α* mRNA levels (Supplemental Fig. 3T, U). Circulating levels of inflammatory markers TNFα and CXCL1 were significantly lower in KD intervention mice compared to HFD continuers (Fig. 4K, L). Circulating IL-1β levels were significantly higher than HFD continuers and IL-6 trended toward an increase (HFD vs. KD $p = 0.0895$) (Fig. 4M, N). Plasma interleukin-5 (IL-5) and IL-2 were not different between diet groups (Fig. 4O, P). In the liver, TNFα levels only trended down in KD mice ($p = 0.0884$) and CXCL1 was not different compared to HFD continuers; however, KD mice had significantly lower liver IL-1β and higher IL-6 levels (Fig. 4Q–T). Liver IL-5 trended up ($p = 0.0976$) in KD mice and interleukin-2 (IL-2) levels were significantly higher (Fig. 4U, V). In all, KD intervention in PCSK9 OE male mice favorably affected hepatic steatosis and inflammation.

### KD intervention slows atherosclerosis progression and lowers chemokine levels in obese, atherosclerotic male mice

Atherosclerotic lesion area was significantly smaller in KD intervention PCSK9 OE mice than HFD continuers, but not reduced to the same extent as the non-cholesterol supplemented chow intervention (Fig. 5A). Percent of neutral lipids in atherosclerotic lesions was not different between groups which is likely due to the advanced nature of the plaque (Fig. 5B) [43]. Compared to maintenance on the HFD, dietary intervention of chow and KD altered the expression of inflammation related genes in the aorta of PCSK9 OE mice. Based on the gene expression, pathway scores were generated by Nanostring; many pathway scores were significantly different, particularly with KD intervention as compared to HFD continuation (Fig. 5D). Both interventions lowered pathway scores for regulation of TLR signaling, ECM organization, complement cascade, and chemokine signaling. Unlike chow intervention, KD additionally reduced CD28 family costimulation pathway scores and increased VEGF, IL-17 signaling, FCERI signaling, cellular response to stress, and apoptosis scores. More singular inflammation-related gene transcripts were differentially expressed compared to HFD in KD (+ 37) than chow (+ 9) intervention, with 23 genes differentially expressed for both KD and chow intervention relative to HFD (Fig. 5E). Some differentially expressed transcripts included reduced expression of *Ccr2* (chow and KD), a macrophage recruitment marker, and chemokine genes *Cxcl1*, *Ccl2*, *Ccl3* (KD only). *Birc2*, previously associated with endothelial integrity and protection from atherosclerosis, was significantly increased specifically in KD intervention mouse aortas (Fig. 5E) [44]. On the other hand, aortas from KD intervention mice had higher expression of *Rac1* which is involved in LDL trafficking in lesion formation [45]. Interestingly, while ketones reportedly inhibit histone deacetylases (HDACs) [46], expression of *Hdac4* was specifically increased in KD mouse aortas (Fig. 5E).

To probe the effects of the altered transcript levels, we measured protein expression of chemokines in

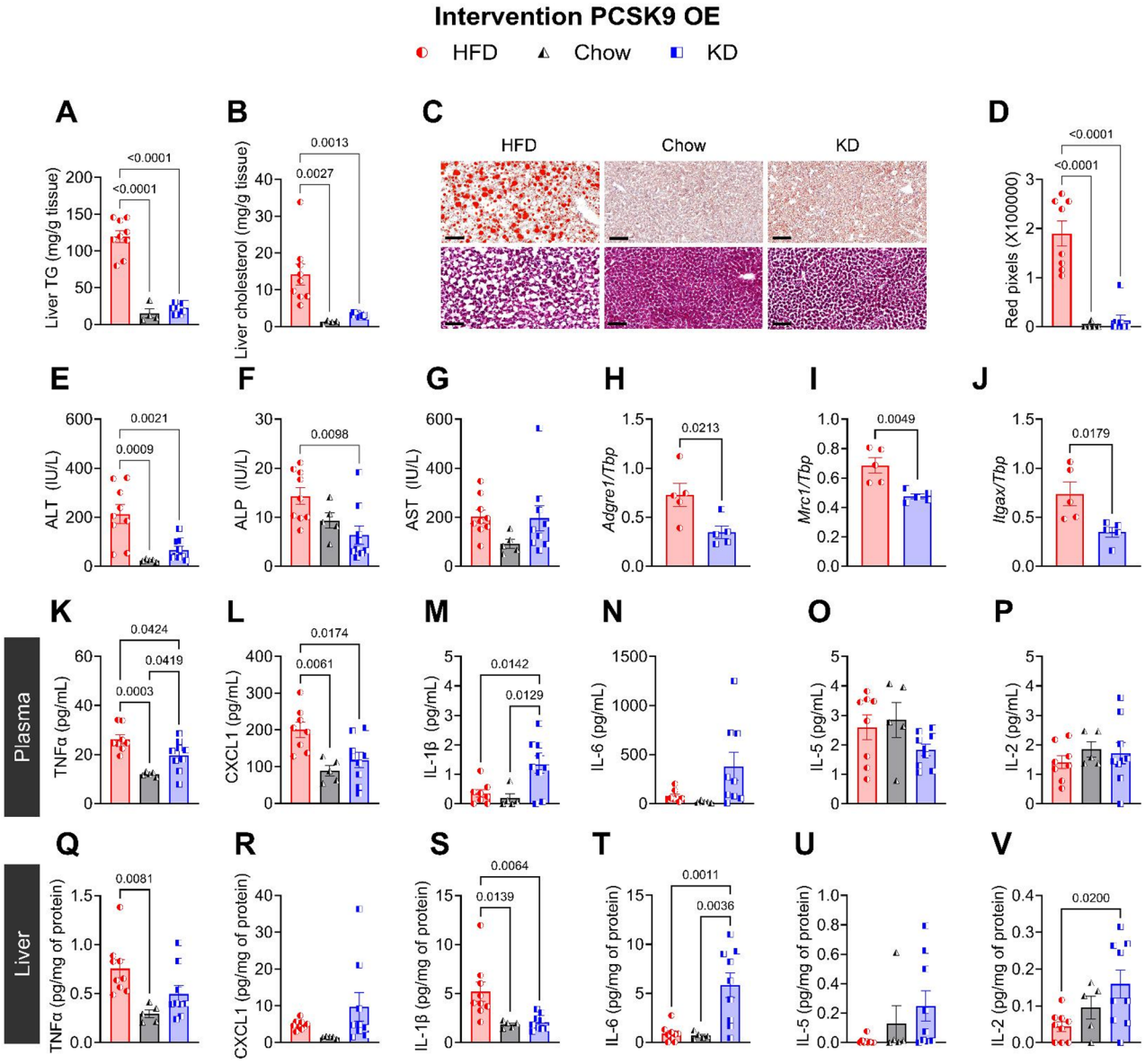


**Fig. 4** KD intervention reduces markers of inflammation and liver lipids in obese, atherosclerotic mice. Male wildtype mice were given PCSK9 AAV injection at 10 weeks old followed by 10 weeks of HFD feeding and then maintenance of HFD or diet intervention with KD or chow for 12 weeks. (**A**, **B**) Endpoint liver triglycerides and liver cholesterol in male intervention mice. (**C**) Representative images of neutral lipid-stained liver slices scale bar represents 100 µm. (**D**) Quantification of neutral lipid staining in liver slices. (**E**, **F**) Plasma liver enzymes in fed endpoint plasma of intervention males. (**H**–**J**) Relative gene expression normalized to *Tbp* in livers from intervention males. (**K**–**P**) Quantification of circulating inflammatory proteins in intervention mice. (**Q**–**V**) Quantification of hepatic inflammatory proteins in intervention mice. Data are presented as mean +/− SEM. P value was determined by one way ANOVA with multiple comparisons or unpaired t-test (**H**-**J**).

plasma and the aorta. Protein levels of aortic CCL3 and CXCL1 were reduced with KD in wildtype mice while CCL2, CCL4, and CXCL2 were not significantly different (Fig. 5F–J). In plasma, CCL3 trended down ($p = 0.065$) in KD intervention PCSK9 OE mice while CXCL1, CCL2, CCL4, and CXCL2 were significantly lower compared to HFD continuers (Fig. 5K–O). Blood analysis during fasting and feeding showed no differences among diet groups in total white blood cell count, neutrophils, lymphocytes, or monocytes (Supplemental Fig. 4). However, basophils, eosinophils, and platelets were lower in KD intervention mice, particularly during fasting (Fig. 5P, Q) (Supplemental Fig. 4). In all, KD intervention in PCSK9 OE males slowed progression of atherosclerosis and reduced plasma and aortic chemokines.

### KD intervention lowers LDL cholesterol only in mice without functional LDL receptor

To evaluate the effects of extreme dietary fat and cholesterol consumption between animal models, we measured

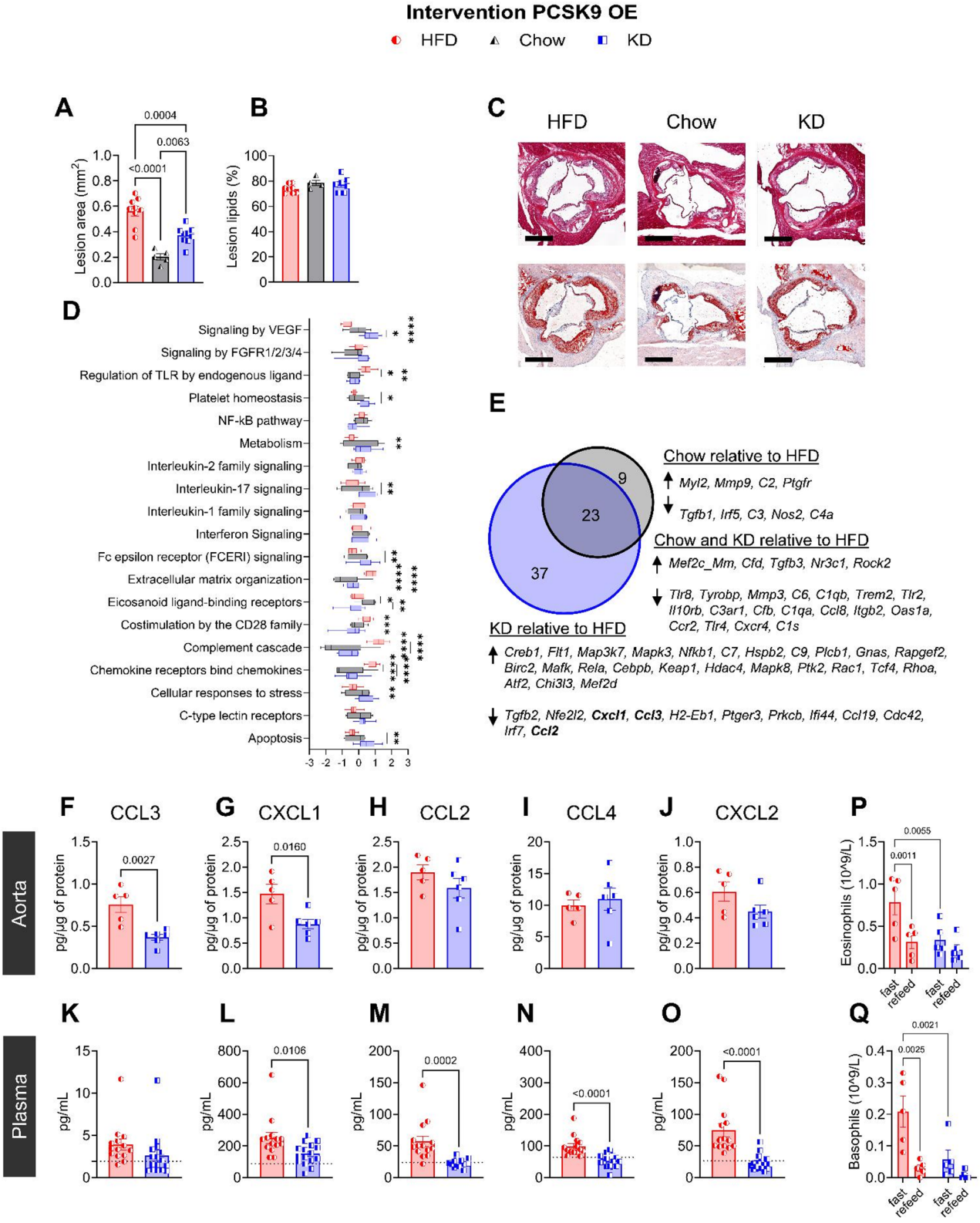


**Fig. 5** (See legend on next page.)

(See figure on previous page.)

**Fig. 5** KD intervention improves lipid parameters and atherosclerotic lesion area in obese, atherosclerotic male mice. Male wildtype mice were given PCSK9 AAV injection at 10 weeks old followed by 10 weeks of HFD feeding and then maintenance of HFD or diet intervention with KD or chow for 12 weeks. (**A**) Quantification of aortic root atherosclerotic lesion area. (**B**) Quantification of neutral lipid staining in atherosclerotic lesion sections. (**C**) Representative images of H & E top. and Oil Red O bottom. -stained aortic sinus sections scale bar represents 500 µm. (**D**) Pathway scores of inflammatory genes pathways in aortic tissue. (**E**) Venn diagram of significantly differentially expressed inflammatory genes in the aortas of KD and chow intervention compared to HFD maintained mice. (**F**–**J**) Quantification of aortic chemokines from mice sacrificed during fasting. (**K**–**O**) Quantification of plasma chemokines from mice sacrificed during fasting. (**P**, **Q**) Blood eosinophils and basophils after 16 h fast and 2 h refeeding of their respective diets in male intervention mice. Data is shown as mean ± SEM. Significance was determined by one way ANOVA with multiple comparisons (**A**, **B**), unpaired t-test (**F**-**O**), or two way ANOVA with multiple comparisons (**P**, **Q**). Dotted line represents the mean of $n = 5$ mice on chow diet intervention.

circulating total, LDL, and HDL cholesterol and triglycerides in intervention wildtype (fed) and PCSK9 OE (fasted) mice. In wildtypes, endpoint circulating total cholesterol, LDL, and HDL were similar between HFD continuers and KD intervention males and females, unlike chow intervention which reduced total, LDL, and HDL cholesterol (Fig. 6A–C, E–G). Circulating triglycerides were significantly higher in KD intervention male and female mice who were sacrificed without fasting (Fig. 6D, H). However, in the atherosclerosis-susceptible PCKS9 OE mice, total plasma cholesterol was reduced with KD intervention compared to continuing the HFD (Fig. 6I). Similarly, plasma LDL was reduced with KD intervention in PCSK9 OE males (Fig. 6J). There were no significant differences between diet groups in fasted plasma HDL or triglycerides in PCSK9 OE mice (Fig. 6K, L).

Since the KD and HFD were both supplemented with the same amount of cholesterol per calorie, and the KD mice had lower liver and circulating cholesterol, particularly in the mice lacking adequate LDL receptor (PCSK9 OE), we evaluated markers of LDLR independent lipoprotein uptake and bile acid synthesis. Transcript levels of LDL receptor related protein-1 (*Lrp1*) were significantly higher in livers from KD intervention PCSK9 OE males than both other diet groups (Fig. 6M). Bile acids are formed through catabolism of cholesterol and serve as a mechanism of cholesterol excretion independent of the LDL receptor [47]. In livers from PCK9 OE male mice sacrificed without fasting, mRNA levels of *Cyp7a1* (*cholesterol 7 alpha-hydroxylase*), the rate limiting enzyme for classical pathway bile acid synthesis, were higher and the bile acid synthesis regulator, *Fxr* (*farnesoid X receptor*), trended toward increase in KD intervention mice compared to HFD continuers ($p = 0.0581$) (Fig. 6N, O). In endpoint fed and fasted plasma, we found no significant difference in total circulating bile acids between diet groups (Fig. 6P, Q). HFD mice had slightly, but insignificantly, higher total bile acids on average in fed state whereas and KD mice had slightly higher bile acids during fasting, indicating a potential "fasting-like" effect of the KD like seen in plasma metabolites (Fig. 1G-P). During fasting, KD-fed mice had higher concentrations of the bile acid HCA, which was undetectable in HFD-fed mice and detectable in 8/12 KD fed mice (Fig. 6R). Chenodeoxycholic acid (CDCA) and its secondary bile acid, lithocholic acid (LCA) were significantly lower in KD intervention relative to HFD mice (Fig. 6S, T).

In wildtype males, KD intervention mice had significantly diminished hepatic PCSK9 protein levels but similar *Lrp1* mRNA levels between diet groups (Fig. 6U, V). In wildtype females, hepatic PCSK9 protein levels were significantly lower than both other diets groups and *Lrp1* transcript levels were elevated (Fig. 6W, X). Thus, while KD intervention drastically reduced circulating cholesterol in PCSK9 OE mice, an atherosclerosis or hypercholesterolemia model may be required to observe improved circulating cholesterol outcomes.

## Discussion

In this study, we used lean (no induction), diet-induced obese (intervention), and diet induced obese, atherosclerotic (PCSK9 OE) models of KD feeding to untangle the effects of both model and control diet on the impact of KD feeding. We observed no improvements in glucose tolerance, in any model, despite high circulating GLP-1 levels after glucose gavage. Obese mice showed no significant changes to stored pancreas lipids. In isolated islets, lean and obese mice had no difference in GSIS among diets but KD dampened glucagon at low glucose levels. Across all models, KD mice had improvements in liver steatosis or liver enzymes with particular improvements in females and PCSK9 OE males who also had total body mass loss. PCSK9 OE KD intervention mice had smaller atherosclerotic lesions, lower levels of many inflammatory markers in circulation and the aorta, and lower total and LDL plasma cholesterol than HFD continuers. If combined with increased bile acid synthesis and non-LDLR mediated, ApoE containing particle uptake, cholesterol could be shunted toward bile acid production and excretion, more effectively overcoming the PCSK9 OE model. However, obese mice with intact LDLR signaling did not recapitulate the beneficial circulating lipid effects.

In line with previous reports, we only observed weight loss with KD intervention in female and not male intervention mice [48]. Additionally, the PCSK9 OE male mice, who gained less weight on the HFD to begin with relative to wildtype males, lost significant weight on the KD intervention. Together, this indicates that only mice

with less severe obesity (atherosclerosis susceptible males, wildtype females) can lose weight and this effect is lost after a certain "point of no return" of metabolic dysfunction/obesity in mice. Importantly, in all models and sexes, KD-fed mice never had significantly different body weight than chow-fed mice. As anticipated with predominance of lipids as fuel, respiratory exchange ratio has previously been reported with prolonged KD feeding [49] and we found that there may be reduced calorie efficiency in the initial weeks of KD intervention. Interestingly, despite the weight loss, females on KD intervention trended toward worse glucose tolerance than HFD mice. Although there were no differences in glucose-stimulated insulin secretion, 4-hour fasted insulin was lower in KD intervention PCSK9 OE males and glucagon levels were suppressed in KD intervention mouse plasma and islets. The differential glucagon levels may be due to the high circulating concentration of BHB [50, 51] which has been shown previously to dampen glucagon in lean and *ob/ob* models of KD [27, 52].

KD intervention mice had significantly higher plasma active GLP-1 levels after a glucose gavage than the other groups, however, it was ineffective at amplifying insulin secretion. This study (Supplemental Fig. 3M), in line with our previous work [18], found increased small intestinal length in male mice on the KD. Greater small intestinal length may result in greater abundance of GLP-1 releasing L-cells which could further increase length due to GLP-1's intestinotrophic effects [42]. Additionally, GLP-2 is co-secreted with GLP-1 as it is derived from prohormone processing of the same proglucagon gene product. Activation of GLP-2R signaling has demonstrated therapeutic efficacy in short bowl syndrome to improve nutrient absorption and gut health [53]. Interestingly, our PCSK9 OE KD intervention mice also had elevated levels of the bile acid HCA (Fig. 6Q). Zheng et al. found that high HCA supplementation increased GLP-1 and improved glucose tolerance in both genetic and diet plus drug (HFD + streptozotocin) induced mouse models of diabetes in a GLP-1R-dependent manner [54]. Further, in PCSK9 OE males, KD intervention elevated IL-6 in liver and plasma which have also been shown to increase GLP-1 secretion from the intestine [55]. Importantly, in our models, KD fed mice do not respond to the extremely high GLP-1 levels to improve glucose tolerance or insulin secretion which may be due to conflicting effects of the GLP-1-increasing factors like IL-6, which is associated with glucose intolerance [33].

Macrophages play an important role in the progression of atherosclerosis; however, in our PCSK9 OE model, gene expression of macrophage markers in the liver were reduced but macrophage gene score in the aorta was unchanged with KD. Despite this, the expression of *Ccr2*, a marker of recruited macrophages [56, 57], was significantly lower in both intervention diets in the aorta compared to HFD maintenance. Blood cell analysis in fasting and refed state did not identify differences in monocytes or lymphocytes, despite reduced CCL2 (aka monocyte chemoattractant protein-1 (MCP-1)) levels. Rather, KD intervention mice had lower eosinophils and basophils, in line with a previous observation that circulating BHB has been negatively associated with eosinophil count in humans [58]. While the method used for monocyte quantification does not differentiate between Ly6CHi, the more proinflammatory, CCR2 expressing monocytes, and Ly6CLo monocytes [59], the lower aortic *Ccr2* levels suggest less recruitment of the proinflammatory monocytes. In line with this, a KD with similar macronutrient proportions reduced macrophage infiltration in a model of kidney fibrosis [60], reinforcing that although total macrophage number in circulation or the aorta may not change at this timepoint, the recruitment of new macrophages to the plaque may be blunted. Chemokines also play an important role in the recruitment of immune cells and systemic inflammation throughout atherosclerosis progression [61]. The mRNA abundance of chemokine genes transcripts and the circulating levels of chemokines were lower in KD intervention mice than HFD PCSK9 OE mice. Previously, Soni and colleagues showed that giving a ketone ester drink prior to lipopolysaccharide injection reduced plasma concentrations of chemokines including CXCL1, CXCL2, CCL2, CCL4 reinforcing that ketone signaling, apart from the extreme macronutrient difference, can regulate inflammation in mice [62].

Previous studies on the effects of KD on atherosclerosis using *ApoE*$^{-/-}$ mice have similarly shown improvements in circulating cholesterol and plaque size relative to HFD but worsening relative to chow [19–21]. Due to the inability of mice to develop atherosclerotic plaque under normal conditions, this (PCSK9 OE) and other studies (*ApoE*$^{-/-}$) use extreme models to allow for atherosclerosis initiation. Importantly, we found that the reduced cholesterol in KD intervention relative to HFD controls in PCSK9 OE mice was not preserved in mice who had intact LDL receptor signaling, indicating that the effects on atherosclerosis would likely not be recapitulated without the extreme model. Interestingly, KD intervention in wildtypes resulted in extremely low hepatic PCSK9 mRNA and protein levels without significant changes to hepatic LDLR protein levels. Loss of functional LDL receptor, the primary means of removing excess cholesterol from circulation, could result in reliance on alternative clearance pathways including bile acid synthesis and excretion for improvements in circulating lipids as shown in a previous study of time restricted feeding in LDLR knockout mice [63]. However, we did not find a significant effect of KD on circulating bile acids levels. This may

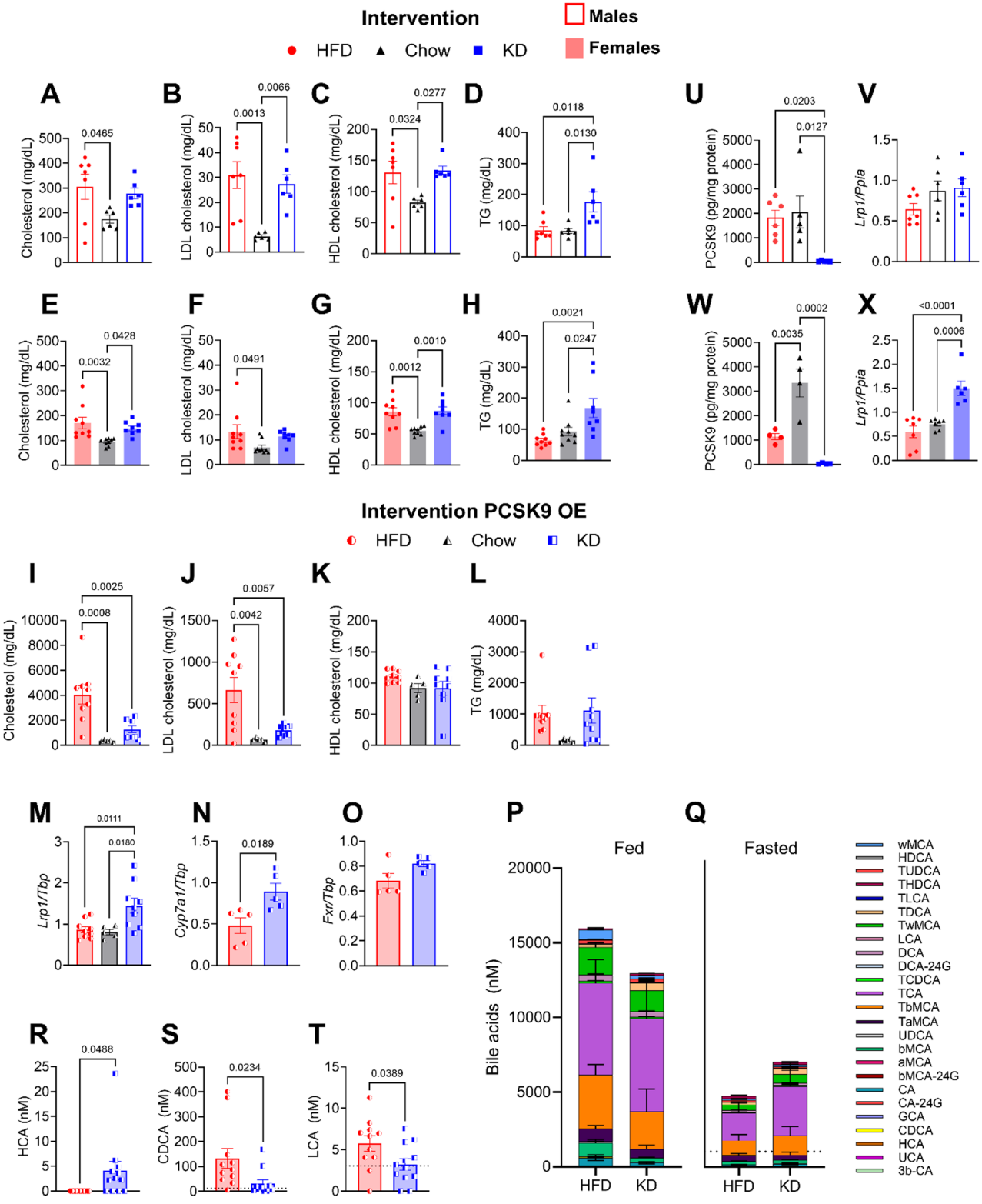


**Fig. 6** (See legend on next page.)

(See figure on previous page.)

**Fig. 6** KD intervention lowers LDL cholesterol only in mice without functional LDL receptor. Wildtype female, male, and PCSK9 OE male mice were given a HFD for 10 weeks followed by KD intervention for 12 weeks. (**A**–**D**) Total cholesterol, LDL, HDL, and triglycerides from week 22 sacrifice fed plasma in wildtype males. (**E**–**H**) Total cholesterol, LDL, HDL, and triglycerides from week 22 sacrifice fed plasma in wildtype females. (**I**–**L**) Total cholesterol, LDL, HDL, and triglycerides from week 22 sacrifice fasted plasma in PCSK9 OE males. (**M**–**O**) Relative gene expression normalized to *Tbp* in livers from PCKS9 OE males. (**P**, **Q**) Total circulating bile acids in endpoint plasma from males PCSK9 OE mice that were sacrificed without (**P**) or with fasting (**Q**). (**R**–**T**) Fasted plasma HCA (**R**), CDCA (**S**), and LCA (**T**) from endpoint PCSK9 OE males. (**U**–**X**) Liver PCSK9 protein (**U**, **W**) and relative gene expression of *Lrp1* (**V**, **X**) in male and female wildtype intervention mice. Data is shown as mean ± SEM. Significance was determined by one way ANOVA with multiple comparisons (**A**–**M**, **U**-**X**) or unpaired t-test (**N**, **O**, **R**–**T**). Dotted line represents the mean of $n = 5$ mice on chow diet intervention.

be due to bile acids being measured after 12 weeks of KD intervention when the majority of bile acid synthesis and excretion of the accumulated cholesterol from the previous HFD feeding would likely have already occurred. The maintenance of lower circulating cholesterol levels despite continued dietary cholesterol intake would have a less striking impact that may not be detectable with the variability of bile acid concentrations. We did, however, find that KD intervention increased *Lrp1* mRNA levels in wildtype females and PCSK9 OE males which may be responsible for increased uptake of ApoE containing particles in this model of atherosclerosis, although it did not result in improved circulating cholesterol levels in the female wildtype mice.

In this study, the KD was designed using the ingredients of the obesogenic HFD. This ingredient-matching was done to avoid the bias of a potentially "healthier" KD with more unsaturated fat content and without supplemented cholesterol. Thus, although the control chow intervention group had greater metabolic improvements including lower circulating cholesterol and liver triglycerides than KD intervention mice, the difference between an ideal KD and lower fat diet can not be ascertained from this work. Regardless, of the superiority of a low fat versus KD, understanding the effects of KD feeding on atherosclerosis are important because of its use in management of glycemic fluctuations and insulin requirement in people living with T2D and type 1 diabetes, and for weight loss in people living with obesity, all of which are at elevated risk for cardiovascular disease [64].

Our KD, like many used in rodent models to induce ketosis, is a more extreme diet than what people on a KD would consume. We chose this model to ensure that mice would have consistently elevated circulating ketones to address the impact not only of macronutrient shift but also the metabolic and signaling effects of ketones [65, 66]. Additionally, although our chow diet can induce weight loss in mice after HFD-induced obesity, it does not have the same ingredients as the other diets and the effect of these very different diet compositions may play a role in the differences between chow intervention and KD intervention. As such, this comparison is not the emphasis of the paper. Our diets also have significantly different caloric densities; however, we did not see significant differences in calorie intake and, where applicable, our results align with a previous study using isocaloric low fat, high fat, and KD [48]. Importantly, our atherosclerosis study was done in exclusively male mice and cannot be generalized to females. Unlike with obesity and glucose tolerance where females have some protection, atherosclerosis is similar among sexes (PCSK9 OE, data not shown) or accelerated in female relative to male mice, dissociating plaque area from metabolic disease generally [67, 68].

## Conclusions

In all, KD feeding consistently improved markers of liver function by lowering liver enzymes or reducing liver lipids. Liver outcomes were most improved in the groups that experienced weight loss, namely atherosclerotic male mice and female obese mice. Cardiovascular risk was also attenuated in male KD intervention PCSK9 OE mice but the cholesterol-lowering effects were restricted to mice with disrupted LDL receptor signaling. KD feeding and intervention did not recover islet function or insulin secretion, despite consistently elevated GLP-1 in response to oral glucose. Together, dietary intervention with this KD can mediate positive effects on lipid metabolism and inflammation in mice, independent of any improvements to glucose handling.

**Abbreviations**

| | |
|---|---|
| ADGRE1 | Adhesion G protein-coupled receptor E1 |
| ALP | Alkaline phosphatase |
| ALT | Alanine transaminase |
| AST | Aspartate aminotransferase |
| BDH1 | D-beta-hydroxybutyrate dehydrogenase |
| BHB | Beta-hydroxybutyrate |
| CDCA | Chenodeoxycholic acid |
| CPT1α | Carnitine palmitoyltransferase I |
| CYP7A1 | Cholesterol 7 alpha-hydroxylase |
| DPP4 | Dipeptidyl peptidase 4 |
| FFA | Free fatty acids |
| FXR | Farnesoid X receptor |
| GC/MS | Gas chromatography mass spectrometry |
| GIP | Glucose dependent insulinotropic polypeptide |
| GLP-1 | Glucagon-like peptide-1 |
| GPCR | G-protein coupled receptor |
| GSIS | Glucose stimulated insulin secretion |
| GTT | Glucose tolerance test |
| HDAC | Histone deacetylase |
| HFD | High fat diet |
| HMGCS2 | 3-hydroxy-3-methylglutaryl-CoA synthase 2 |
| IL-1β | Interleukin 1β |
| IL-6 | Interleukin 6 |
| ITGAX | Integrin subunit alpha X |
| KC-GRO/CXCL1 | Keratinocyte chemoattractant/growth-regulated oncogene |
| KD | Ketogenic diet |

| | |
|---|---|
| LCA | Lithocholic acid |
| LDL | Low-density lipoprotein |
| LRP-1 | LDL receptor-related protein-1 |
| MCP-1/CCL2 | Monocyte chemoattractant protein 1 |
| Mrc1 | Mannose receptor C-type 1 |
| OE | Overexpression |
| PCSK9 | Proprotein convertase subtilisin/kexin type 9 |
| T2D | Type 2 diabetes |
| TNFα | Tumor necrosis factor α |

## Supplementary Information

The online version contains supplementary material available at https://doi.org/10.1186/s12933-025-03046-3.

Supplementary Material 1

**Acknowledgements**
The authors would like to thank Xiaoling Zhao, Evgenia Fadzeyeva, Antonio Hanson, Nicole Travis, and Brian Le for their technical assistance. Thank you to Morgan Fullerton, Kyoung-Han Kim, and Wenbin Liang for advising the direction of these studies.

**Author contributions**
Conceptualization, E.E.M, C.A.A.L.; methodology, C.A.A.L., M.A.N., N.M.M, I.L.S.; Investigation, C.A.A.L, M.A.N., N.M.M, E.C., N.A.T; writing—original draft, C.A.A.L.; writing—review & editing, C.A.A.L., A.M., E.E.M.; funding acquisition, E.E.M.; resources, E.E.M.; supervision, E.E.M.

**Funding**
This work was supported by the Diabetes Canada End Diabetes grant (RN470374-OG3-21-5591-EM). C.A.A.L. was supported by the University of Ottawa Heart Institute Cardiac Endowment Fund, Ontario Graduate Scholarship, and the CIRTN R2FIC NSERC-CREATE Training Program. N.M.M was supported by the Canadian Institutes of Health Research Doctoral award. N.A.T. was supported by the University of Ottawa Heart Institute Cardiac Endowment Fund.

**Data availability**
All data reported in this paper will be shared by the authors upon request.

## Declarations

**Competing interests**
The authors declare no competing interests.

**Author details**
[1]Department of Biochemistry, Microbiology and Immunology, Faculty of Medicine, The University of Ottawa, 451 Smyth Road, room 4103, ON K1H 8M5 Ottawa, Canada
[2]The University of Ottawa Heart Institute, 40 Ruskin Street, Ottawa, ON K1Y4W7, Canada
[3]Department of Chemistry and Biomolecular Science, Faculty of Science, The University of Ottawa, K1N 6N5 Ottawa, Canada
[4]Centre for Infection, Immunity and Inflammation, The University of Ottawa, 451 Smyth Rd, Ottawa, ON K1H 8M5, Canada
[5]Present address: Ottawa Institute of Systems Biology, University of Ottawa, 451 Smyth Road, Ottawa, Canada

Received: 3 October 2025 / Accepted: 12 December 2025
Published online: 03 January 2026

**References**

1. Feinman RD, Pogozelski WK, Astrup A, Bernstein RK, Fine EJ, Westman EC, et al. Dietary carbohydrate restriction as the first approach in diabetes management: critical review and evidence base. Nutrition. 2015;31(1):1–13.
2. Lu VB, Gribble FM, Reimann F. Nutrient-Induced cellular mechanisms of gut hormone secretion. Nutrients. 2021;13(3):883.
3. Baggio LL, Drucker DJ. Biology of incretins: GLP-1 and GIP. Gastroenterology. 2007;132(6):2131–57.
4. Ghislain J, Poitout V. Targeting lipid GPCRs to treat type 2 diabetes mellitus—progress and challenges. Nat Rev Endocrinol. 2021;17(3):162–75.
5. Tabatabaei Dakhili SA, Yang K, Locatelli CAA, Saed CT, Greenwell AA, Chan JSF, et al. Ketone ester administration improves glycemia in obese mice. Am J Physiol Cell Physiol. 2023 Sept;325(3):C750–7.
6. Dietary fat and its relation to heart attacks and strokes. Report by the central committee for medical and community program of the American heart association. JAMA. 1961;175:389–91. https://doi.org/10.1161/01.CIR.23.1.133}
7. Mensink RP, Katan MB. Effect of dietary fatty acids on serum lipids and lipoproteins. A meta-analysis of 27 trials. Arterioscler Thromb. 1992;12(8):911–9.
8. Soto-Mota A, Norwitz NG, Manubolu VS, Kinninger A, Wood TR, Earls J et al. Plaque begets Plaque, ApoB does not: longitudinal data from the KETO-CTA trial. JACC: Adv. 2025;101686.
9. Libby P. Interleukin-1 beta as a target for atherosclerosis therapy: the biological basis of CANTOS and beyond. J Am Coll Cardiol. 2017;70(18):2278–89.
10. Boisvert WA, Rose DM, Johnson KA, Fuentes ME, Lira SA, Curtiss LK, et al. Up-regulated expression of the CXCR2 ligand KC/GRO-alpha in atherosclerotic lesions plays a central role in macrophage accumulation and lesion progression. Am J Pathol. 2006;168(4):1385–95.
11. Gosling J, Slaymaker S, Gu L, Tseng S, Zlot CH, Young SG, et al. MCP-1 deficiency reduces susceptibility to atherosclerosis in mice that overexpress human apolipoprotein B. J Clin Invest. 1999;103(6):773–8.
12. Hartman J, Frishman WH. Inflammation and atherosclerosis: A review of the role of Interleukin-6 in the development of atherosclerosis and the potential for targeted drug therapy. Cardiol Rev. 2014 June;22(3):147.
13. Reiss AB, Siegart NM, De Leon J. Interleukin-6 in atherosclerosis: atherogenic or atheroprotective? Clin Lipidol. 2017;12(1):14–23.
14. Brånén L, Hovgaard L, Nitulescu M, Bengtsson E, Nilsson J, Jovinge S. Inhibition of tumor necrosis factor-α reduces atherosclerosis in apolipoprotein E knockout mice. Arterioscler Thromb Vasc Biol. 2004;24(11):2137–42.
15. Goldberg IJ, Ibrahim N, Bredefeld C, Foo S, Lim V, Gutman D, et al. Ketogenic diets, not for everyone. J Clin Lipidol. 2021;15(1):61–7.
16. Naveh N, Avidan Y, Zafrir B. Extreme hypercholesterolemia following a ketogenic diet: exaggerated response to an increasingly popular diet. Cureus. 2023;15(8):e43683.
17. Omar A, Fishberg R, Alam L. *Ketogenic diets exacerbating hypercholesterolemia in APOE variants and APOB mutations-potential role for measuring intestinal absorption of lipids. Journal of Clinical Lipidology. 2022;16(3, Supplement):e60–1.
18. Morrow NM, Locatelli CAA, Trzaskalski NA, Klein CT, Hanson AA, Alhadi H, et al. Adaptation to short-term extreme fat consumption alters intestinal lipid handling in male and female mice. Biochimica et biophysica acta (BBA). Mol Cell Biology Lipids. 2022;1867(11):159208.
19. da Silva IV, Gullette S, Florindo C, Huang NK, Neuberger T, Ross AC, et al. The effect of nutritional ketosis on aquaporin expression in apolipoprotein E-deficient mice: potential implications for energy homeostasis. Biomedicines. 2022;10(5):1159.
20. Castro R, Whalen CA, Gullette S, Mattie FJ, Florindo C, Heil SG, et al. A hypomethylating ketogenic diet in apolipoprotein e-deficient mice: a pilot study on vascular effects and specific epigenetic changes. Nutrients. 2021;13(10):3576.
21. Castro R, Kalecký K, Huang NK, Petersen K, Singh V, Ross AC, et al. A very-low carbohydrate content in a high-fat diet modifies the plasma metabolome and impacts systemic inflammation and experimental atherosclerosis. J Nutr Biochem. 2024;126:109562.
22. Zhang SJ, Li ZH, Zhang YD, Chen J, Li Y, Wu FQ, et al. Ketone body 3-hydroxybutyrate ameliorates atherosclerosis via receptor Gpr109a-mediated calcium influx. Adv Sci (Weinh). 2021;8(9):2003410.
23. Kim ER, Kim SR, Cho W, Lee SG, Kim SH, Kim JH, et al. Short term isocaloric ketogenic diet modulates NLRP3 inflammasome via B-hydroxybutyrate and fibroblast growth factor 21. Front Immunol. 2022;13:843520.
24. Youm YH, Nguyen KY, Grant RW, Goldberg EL, Bodogai M, Kim D, et al. Ketone body β-hydroxybutyrate blocks the NLRP3 inflammasome-mediated inflammatory disease. Nat Med. 2015;21(3):263–9.
25. Locatelli CAA, Mulvihill EE. Islet health, hormone secretion, and insulin responsivity with low-carbohydrate feeding in diabetes. Metabolites. 2020;10(11):455.

26. Nasser S, Solé T, Vega N, Thomas T, Balcerczyk A, Strigini M, et al. Ketogenic diet administration to mice after a high-fat-diet regimen promotes weight loss, glycemic normalization and induces adaptations of ketogenic pathways in liver and kidney. Mol Metabolism. 2022;65:101578.
27. Badman MK, Kennedy AR, Adams AC, Pissios P, Maratos-Flier E. A very low carbohydrate ketogenic diet improves glucose tolerance in ob/ob mice independently of weight loss. Badman MK, editor. American Journal of Physiology Endocrinology and Metabolism. 2009;297(5):E1197–204.
28. Mardinoglu A, Wu H, Bjornson E, Zhang C, Hakkarainen A, Räsänen SM, et al. An integrated understanding of the rapid metabolic benefits of a carbohydrate-restricted diet on hepatic steatosis in humans. Cell Metabol. 2018;27(3):559–e5715.
29. Tendler D, Lin S, Yancy WS, Mavropoulos J, Sylvestre P, Rockey DC, et al. The effect of a low-carbohydrate, ketogenic diet on nonalcoholic fatty liver disease: a pilot study. Dig Dis Sci. 2007;52(2):589–93.
30. Luukkonen PK, Dufour S, Lyu K, Zhang XM, Hakkarainen A, Lehtimäki TE et al. Effect of a ketogenic diet on hepatic steatosis and hepatic mitochondrial metabolism in nonalcoholic fatty liver disease. Proceedings of the National Academy of Sciences. 2020;117(13):7347–54.
31. Garbow JR, Doherty JM, Schugar RC, Travers S, Weber ML, Wentz AE, et al. Hepatic steatosis, inflammation, and ER stress in mice maintained long term on a very low-carbohydrate ketogenic diet. Am J Physiol - Gastrointest Liver Physiol. 2011;300(6):956–67.
32. Sprankle KW, Knappenberger MA, Locke EJ, Thompson JH, Vinovrski MF, Knapsack K, et al. Sex- and age-specific differences in mice fed a ketogenic diet. Nutrients. 2024;16(16):2731.
33. Long F, Bhatti MR, Kellenberger A, Sun W, Modica S, Höring M, et al. A low-carbohydrate diet induces hepatic insulin resistance and metabolic associated fatty liver disease in mice. Mol Metabolism. 2023;69:101675.
34. You Y, Huang Y, Wang X, Ni H, Ma Q, Ran H, et al. Ketogenic diet time-dependently prevents NAFLD through upregulating the expression of antioxidant protein metallothionein-2. Clin Nutr. 2024;43(6):1475–87.
35. Bjørklund MM, Hollensen AK, Hagensen MK, Dagnæs-Hansen F, Christoffersen C, Mikkelsen JG, et al. Induction of atherosclerosis in mice and hamsters without germline genetic engineering. Circul Res. 2014;114(11):1684–9.
36. Morissette A, de Wouters d'Oplinter A, Andre DM, Lavoie M, Marcotte B, Varin TV, et al. Rebaudioside D decreases adiposity and hepatic lipid accumulation in a mouse model of obesity. Sci Rep. 2024;14:3077.
37. Burnett JR, Wilcox LJ, Telford DE, Kleinstiver SJ, Barrett PHR, Newton RS et al. Inhibition of HMG-CoA reductase by atorvastatin decreases both VLDL and LDL apolipoprotein B production in miniature pigs. Arteriosclerosis, Thrombosis, and Vascular Biology. 1997;17(11):2589–600.
38. Patel R, Patel M, Tsai R, Lin V, Bookout AL, Zhang Y, et al. LXRβ is required for glucocorticoid-induced hyperglycemia and hepatosteatosis in mice. J Clin Invest. 2011;121(1):431–41.
39. Fu J, Liu S, Li M, Guo F, Wu X, Hu J, et al. Optimal fasting duration for mice as assessed by metabolic status. Sci Rep. 2024;14(1):21509.
40. Stahel P, Xiao C, Davis X, Tso P, Lewis GF. Glucose and glucagon-like peptide-2 mobilize intestinal triglyceride by distinct mechanisms. Arterioscler Thromb Vasc Biol. 2019;39(8):1565–73.
41. Xiao C, Stahel P, Carreiro AL, Hung YH, Dash S, Bookman I, et al. Oral glucose mobilizes triglyceride stores from the human intestine. Cell Mol Gastroenterol Hepatol. 2018;7(2):313–37.
42. Koehler JA, Baggio LL, Yusta B, Longuet C, Rowland KJ, Cao X, et al. GLP-1R agonists promote normal and neoplastic intestinal growth through mechanisms requiring *Fgf7*. Cell Metabol. 2015;21(3):379–91.
43. Rasheed A, Robichaud S, Nguyen MA, Geoffrion M, Wyatt H, Cottee ML, et al. Arteriosclerosis Thromb Vas Biol. 2020;40(5):1155–67.
44. Santoro MM, Samuel T, Mitchell T, Reed JC, Stainier DYR. Birc2 (clap1) regulates endothelial cell integrity and blood vessel homeostasis. Nat Genet. 2007;39(11):1397–402.
45. Huang L, Chambliss KL, Gao X, Yuhanna IS, Behling-Kelly E, Bergaya S, et al. SR-B1 drives endothelial cell LDL transcytosis via DOCK4 to promote atherosclerosis. Nature. 2019;569(7757):565–9.
46. Shimazu T, Hirschey MD, Newman J, He W, Moan NL, Grueter CA, et al. Suppression of oxidative stress by β-hydroxybutyrate, an endogenous histone deacetylase inhibitor. Science. 2013;339(6116):211–4.
47. Chiang JYL, Ferrell JM, Wu Y, Boehme S. Bile acid and cholesterol metabolism in atherosclerotic cardiovascular disease and therapy. Cardiol Plus. 2020;5(4):159–70.
48. Greenwell AA, Saed CT, Tabatabaei Dakhili SA, Ho KL, Gopal K, Chan JSF, et al. An isoproteic cocoa butter-based ketogenic diet fails to improve glucose homeostasis and promote weight loss in obese mice. Am J Physiol Endocrinol Metabol. 2022;323(1):E8–20.
49. Gallop MR, Vieira RFL, Mower PD, Matsuzaki ET, Liou W, Smart FE, et al. A long-term ketogenic diet causes hyperlipidemia, liver dysfunction, and glucose intolerance from impaired insulin secretion in mice. Sci Adv. 2025;19(38):eadx2752.
50. Banerjee R, Zhu Y, Brownrigg GP, Moravcova R, Rogalski JC, Foster LJ, et al. Beta-Hydroxybutyrate promotes basal insulin secretion while decreasing glucagon secretion in mouse and human islets. Endocrinology. 2024;165(8):bqae079.
51. Morrison CD, Hill CM, DuVall MA, Coulter CE, Gosey JL, Herrera MJ, et al. Consuming a ketogenic diet leads to altered hypoglycemiccounter-regulation in mice. J Diabetes Complicat. 2020;34(5):107557.
52. Jornayvaz FR, Jurczak MJ, Lee HY, Birkenfeld AL, Frederick DW, Zhang D, et al. A high-fat, ketogenic diet causes hepatic insulin resistance in mice, despite increasing energy expenditure and preventing weight gain. Am J Physiol - Endocrinol Metabolism. 2010;299(5):808–15.
53. Drucker DJ. The discovery of GLP-2 and development of teduglutide for short bowel syndrome. ACS Pharmacol Transl Sci. 2019;2(2):134–42.
54. Zheng X, Chen T, Jiang R, Zhao A, Wu Q, Kuang J, et al. Hyocholic acid species improve glucose homeostasis through a distinct TGR5 and FXR signaling mechanism. Cell Metabol. 2021;33(4):791–e8037.
55. Kahles F, Meyer C, Möllmann J, Diebold S, Findeisen HM, Lebherz C, et al. GLP-1 secretion is increased by inflammatory stimuli in an IL-6–Dependent Manner, leading to hyperinsulinemia and blood glucose Lowering. Diabetes. 2014;15(10):3221–9.
56. Dick SA, Macklin JA, Nejat S, Momen A, Clemente-Casares X, Althagafi MG, et al. Self-renewing resident cardiac macrophages limit adverse remodeling following myocardial infarction. Nat Immunol. 2019;20(1):29–39.
57. Boniakowski AE, Kimball AS, Joshi A, Schaller M, Davis FM, denDekker A, et al. Macrophage chemokine receptor CCR2 plays a crucial role in macrophage recruitment and regulated inflammation in wound healing. Eur J Immunol. 2018;48(9):1445–55.
58. Nishi K, Matsumoto H, Tashima N, Terada S, Nomura N, Kogo M, et al. Impacts of lipid-related metabolites, adiposity, and genetic background on blood eosinophil counts: the Nagahama study. Sci Rep. 2021;28:11:15373.
59. Geissmann F, Jung S, Littman DR. Blood Monocytes Consist of Two Principal Subsets with Distinct Migratory Properties. Immunity. 2003;19(1):71–82.
60. Qiu Y, Hu X, Xu C, Lu C, Cao R, Xie Y, et al. Ketogenic diet alleviates renal fibrosis in mice by enhancing fatty acid oxidation through the free fatty acid receptor 3 pathway. Front Nutr. 2023;10:1127845.
61. Márquez AB, van der Vorst EPC, Maas SL. Key chemokine pathways in atherosclerosis and their therapeutic potential. J Clin Med. 2021;10(17):3825.
62. Soni S, Martens MD, Takahara S, Silver HL, Maayah ZH, Ussher JR, et al. Exogenous ketone ester administration attenuates systemic inflammation and reduces organ damage in a lipopolysaccharide model of sepsis. Biochim Biophys Acta Mol Basis Dis. 2022;1868(11):166507.
63. Chaix A, Lin T, Ramms B, Cutler RG, Le T, Lopez C et al. Time-Restricted feeding reduces atherosclerosis in LDLR KO mice but not in ApoE knockout mice. Arteriosclerosis, Thrombosis, and vascular biology. 2024 Sept;44(9):2069–87.
64. Lennerz BS, Koutnik AP, Azova S, Wolfsdorf JI, Ludwig DS. Carbohydrate restriction for diabetes: rediscovering centuries-old wisdom. J Clin Invest. 2021;131(1):e142246.
65. Puchalska P, Crawford PA. Multi-dimensional roles of ketone bodies in fuel metabolism, signaling, and therapeutics. Cell Metabol. 2017;25(2):262–84.
66. Puchalska P, Crawford PA. Metabolic and signaling roles of ketone bodies in health and disease. Annu Rev Nutr. 2021;41:49–77.
67. Smith DD, Tan X, Tawfik O, Milne G, Stechschulte DJ, Dileepan KN. Increased aortic atherosclerotic plaque development in female Apolipoprotein E-null mice is associated with elevated thromboxane A2 and decreased Prostacyclin production. J Physiol Pharmacol. 2010 June;61(3):309–16.
68. Smit V, de Mol J, Kleijn MNAB, Depuydt MAC, de Winther MPJ, Bot I, et al. Sexual dimorphism in atherosclerotic plaques of aged Ldlr-/- mice. Immun Ageing. 2024;21(1):27.


## Publisher's note